

Shortcuts to adiabatic rotation of a two-ion chain

Ander Tobalina

Departament of Physical Chemistry, University of the Basque Country (UPV/EHU),
Apdo. 644, 48080 Bilbao, Spain

Juan Gonzalo Muga

Departament of Physical Chemistry, University of the Basque Country (UPV/EHU),
Apdo. 644, 48080 Bilbao, Spain

Ion Lizuain

Department of Applied Mathematics, University of the Basque Country UPV/EHU,
Donostia-San Sebastian, Spain

Mikel Palmero

E-mail: mikel.palmero@ehu.eus

Department of Applied Physics, University of the Basque Country (UPV/EHU),
48013 Bilbao, Spain

Abstract. We inverse engineer fast rotations of a linear trap with two ions for a predetermined rotation angle and time, avoiding final excitation. Different approaches are analyzed and compared when the ions are of the same species or of different species. The separability into dynamical normal modes for equal ions in a common harmonic trap, or for different ions in non-harmonic traps with up to quartic terms allows for simpler computations of the rotation protocols. For non-separable scenarios, in particular for different ions in a harmonic trap, rotation protocols are also found using more costly numerical optimisations.

1. Introduction

Trapped ions stand out as a flexible architecture to control internal and/or motional states and dynamics for fundamental research of quantum phenomena and technological applications. Pure motional control without internal state transitions is in particular crucial in proposals of two-qubit gates, see e.g. [1], or interferometry [2, 3, 4], as well as to scale up the number of ions for quantum information processing [5, 6, 7, 8, 9, 10, 11, 12]. The toolbox of basic operations induced by controlling the voltage of electrodes in different Paul trap configurations or detuned laser fields includes transport, expansions and compressions, separation and merging of ion chains, and rotations, the latter being the central topic of this work.

Specific motivations to implement rotations are: reordering an ion chain (to scale up quantum information processing or to locate cooling ions at appropriate positions) [13, 14]; rotation sensing [2]; different simulations (e.g. of black holes [15] or diatomic molecules [16]); probing the exchange phase of quantum statistics [17]; or sorting ions according to charge and mass [18].

Trap rotations, to impart some angular momentum to an ion or ion chain, or to reorient the longitudinal axis of the trap, have been implemented in experiments with improving accuracy [13, 16, 14, 19], and investigated theoretically [20, 21].

Motional control operations, and rotations in particular, need in most applications to be fast, relative to adiabatic dynamics, but also gentle, avoiding final excitations, two requirements met with shortcut to adiabaticity (STA) driving protocols [22]. There are different STA techniques but, for trapped ion driving, STA invariant-based inverse engineering has proven useful [1, 3, 4, 21, 23, 24, 25, 26, 27, 28, 29, 30, 31], also to design trap rotations for a single ion [20].

In this paper we extend to a two-ion chain the design of STA 1D-trap rotations done in reference [20]. Our aim is to inverse engineer the rotation angle to implement a fast process, free from final excitations. The work in reference [20] was indeed presented as a preliminary step towards the more complex scenario of the chain rotation, which allows for different, and surely more relevant applications, in particular reordering. Engineering the two-ion rotation also entails non-trivial technical complications due to the increase in the number of equations to be solved, and also because, for some configurations, in particular for two different species in a harmonic trap, there is not in general a point-transformation that provides independent dynamical normal modes [21]‡. Inverse engineering is much easier -to describe the motion and with respect to computational time- for independent modes than for a system which is not separable by point-transformations.§

We introduce now the basic model. We opt for a cavalier, idealised modelling where the trap is assumed for simplicity to be tightly confined in the radial direction, as depicted in figure 1, i.e., we leave aside peculiarities of the experimental settings, such as micromotion effects and detailed electrode configurations, that may vary significantly among different traps. Our solutions will therefore be guiding starting points for a realistic implementation [19, 33].

The trapping line rotates in a horizontal plane in a time t_f up to a predetermined final angle, $\theta_f = \pi$ in all examples. We first find the classical Hamiltonian from the corresponding Lagrangian and then quantise the result. Let s_i , $i = 1, 2$, denote the points on the line where each ion lays. s_i may take positive and negative values. The

‡ “Dynamical normal modes” generalise regular (static) normal modes. They are independent concerted motions represented by harmonic oscillators with time-dependent parameters [21, 25], generally with a time-dependent oscillation frequency.

§ Separability by non-point transformations is possible in principle but it is considerably more involved in terms of its interpretation and practical use. Its application to inverse engineer one-particle rotations in anisotropic traps was explored in [32] under some strong restrictions in process timing and rotation speed.

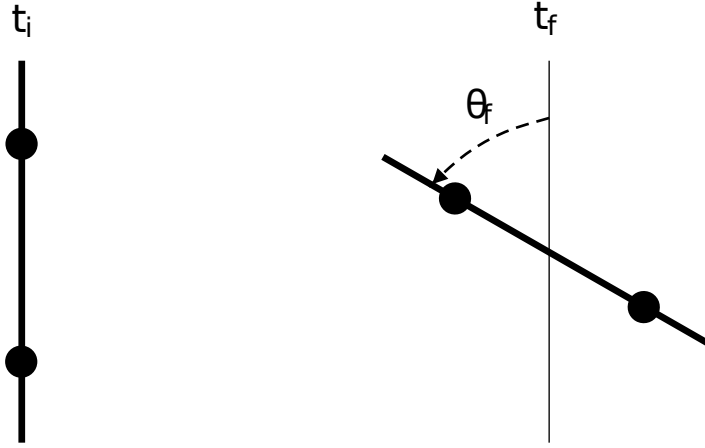


Figure 1. (Color online) Schematic representation of the rotation of two ions confined along a line rotated by an angle θ_f in a time time t_f .

Cartesian (lab frame) components of a trajectory $s_i(t)$ are $x_i = x_i(s, t)$, $y_i = y_i(s, t)$,

$$x_i = s_i \cos(\theta), \quad y_i = s_i \sin(\theta), \quad (1)$$

where $\theta = \theta(t)$ is the rotation angle. For two different ions in a common trap potential $f(s_i)$ the Lagrangian is (we have considered that the magnetic interaction between the two moving charges can be safely neglected, see Appendix A)

$$L = \sum_{i=1,2} \left[\frac{m_i \dot{s}_i^2}{2} - f(s_i) + \frac{m_i \dot{\theta}^2}{2} s_i^2 \right] - \frac{C_c}{s_2 - s_1}, \quad (2)$$

with corresponding Hamiltonian

$$H = \frac{p_1^2}{2m_1} + \frac{p_2^2}{2m_2} + V, \quad (3)$$

$$V = \sum_{i=1,2} \left[f(s_i) - \frac{m_i \dot{\theta}^2}{2} s_i^2 \right] + \frac{C_c}{s_2 - s_1}. \quad (4)$$

In the Coulomb repulsion term $C_c = e^2/(4\pi\epsilon_0)$, where ϵ_0 is the vacuum permittivity, and e the electric charge of the electron.

The equilibrium positions $\{s_i^{(0)}\}$ of the ions are found by solving the set of equations $\{\partial V/\partial s_i = 0\}$. Since different external traps may be considered, the following equations are for a generic V , the results for the simple harmonic trap are given later in section 2.1.

We define the equilibrium distance between ions as

$$d = s_2^{(0)} - s_1^{(0)} \quad (5)$$

and expand V around the equilibrium positions, keeping terms up to second order. Using mass-weighted coordinates $\tilde{s}_i = \sqrt{m_i} s_i$ and momenta $\tilde{p}_i = p_i / \sqrt{m_i}$, H is simplified to the quadratic form

$$H = \frac{\tilde{p}_1^2}{2} + \frac{\tilde{p}_2^2}{2} + (\tilde{s}_1 - s_1^{(0)}, \tilde{s}_2 - s_2^{(0)}) \mathbf{v} \begin{pmatrix} \tilde{s}_1 - s_1^{(0)} \\ \tilde{s}_2 - s_2^{(0)} \end{pmatrix}, \quad (6)$$

where the matrix \mathbf{v} has elements $v_{ij} = \frac{1}{\sqrt{m_i m_j}} \frac{\partial^2 V}{\partial s_i \partial s_j} \Big|_{\{s_i, s_j\} = \{s_i^{(0)}, s_j^{(0)}\}}$.

2. Diagonalisation and dynamical normal modes: setting the equations

We may try to decouple the dynamics by diagonalising \mathbf{v} . As explained in reference [21], moving to a frame defined by the eigenvectors of \mathbf{v} leads, after a classical canonical transformation or, equivalently, quantum unitary transformation, to the following effective Hamiltonian [21]

$$H' = \sum_{\nu=\pm} \left[\frac{p_\nu^2}{2} + \frac{\Omega_\nu^2}{2} \left(s_\nu + \frac{\dot{p}_{0\nu}}{\Omega_\nu^2} \right)^2 \right] - \dot{\mu}(s_- p_+ - s_+ p_-), \quad (7)$$

where μ is the tilting angle of the potential in configuration space defined by the relation

$$\tan 2\mu = \frac{2v_{12}}{v_{11} - v_{22}}, \quad (8)$$

and the momentum shifts

$$p_{0+} = \dot{s}_1^{(0)} \sqrt{m_1} \cos \mu + \dot{s}_2^{(0)} \sqrt{m_2} \sin \mu, \quad (9)$$

$$p_{0-} = -\dot{s}_1^{(0)} \sqrt{m_1} \sin \mu + \dot{s}_2^{(0)} \sqrt{m_2} \cos \mu, \quad (10)$$

have been defined. The coordinates that diagonalise \mathbf{v} are

$$s_+ = \sqrt{m_1}(s_1 - s_1^{(0)}) \cos \mu + \sqrt{m_2}(s_2 - s_2^{(0)}) \sin \mu, \quad (11)$$

$$s_- = -\sqrt{m_1}(s_1 - s_1^{(0)}) \sin \mu + \sqrt{m_2}(s_2 - s_2^{(0)}) \cos \mu, \quad (12)$$

with conjugate momenta

$$p_+ = \frac{\cos \mu}{\sqrt{m_1}} p_1 + \frac{\sin \mu}{\sqrt{m_2}} p_2, \quad (13)$$

$$p_- = -\frac{\sin \mu}{\sqrt{m_1}} p_1 + \frac{\cos \mu}{\sqrt{m_2}} p_2. \quad (14)$$

The squares of the frequencies are

$$\begin{aligned} \Omega_+^2 &= v_{11} \cos^2 \mu + v_{22} \sin^2 \mu + v_{12} \sin 2\mu, \\ \Omega_-^2 &= v_{11} \sin^2 \mu + v_{22} \cos^2 \mu - v_{12} \sin 2\mu. \end{aligned} \quad (15)$$

s_{\pm} describe independent, dynamical normal modes whenever μ is time independent, see equation (7). In a quantum scenario this means that any wave-function dynamics can be decomposed in terms of the dynamics of two independent harmonic oscillators with time-dependent parameters. Different scenarios to achieve this decoupling are considered in the following.

2.1. Results for the harmonic trap

For the common harmonic external potential with spring constant k , $f(s_i) = ks_i^2/2$, which is the only configuration considered hereafter in the main text, the potential (4) takes the form

$$V = \frac{1}{2}u_1 s_1^2 + \frac{1}{2}u_2 s_2^2 + \frac{C_c}{s_2 - s_1}, \quad (16)$$

where

$$u_i = m_i(\omega_i^2 - \dot{\theta}^2), \quad m_i\omega_i^2 = k. \quad (17)$$

The u_i are effective spring constants affected by the rotation speed. Unless $m_1 = m_2$, they are different for both ions. With this V we find the explicit relations

$$\begin{aligned} s_i^{(0)} &= - \left[\frac{C_c u_j^2}{u_i(u_i + u_j)^2} \right]^{1/3}, \quad i \neq j, \\ d &= \left[\frac{C_c(u_1 + u_2)}{u_1 u_2} \right]^{1/3}, \\ \mathbf{v} &= \begin{pmatrix} \frac{2C_c + u_1}{m_1} & -\frac{2C_c}{d^3 \sqrt{m_1 m_2}} \\ -\frac{2C_c}{d^3 \sqrt{m_1 m_2}} & \frac{\frac{2C_c}{d^3} + u_2}{m_2} \end{pmatrix}, \\ \tan 2\mu &= \frac{4C_c \sqrt{m_1 m_2}}{(m_1 - m_2)(2C_c + d^3 k)}. \end{aligned} \quad (18)$$

3. Equal ions

If the ions are equal, $m_1 = m_2 = m$, the tilting angle takes the constant value $\mu = -\pi/4$. The decoupling condition is therefore identically satisfied at all times. Also, $u_1 = u_2 = u = m\omega^2$, with

$$\omega^2 = \omega_0^2 - \dot{\theta}^2 \quad (19)$$

and ω_0 constant. The angular velocity of the rotation $\dot{\theta}(t)$ could be negative at some intervals, whereas ω^2 may also be positive or negative. The equilibrium positions are simplified to

$$s_2^{(0)} = -s_1^{(0)} = \frac{x_0}{2} \quad \text{with} \quad x_0 = \left(\frac{2C_c}{m\omega^2} \right)^{1/3}, \quad (20)$$

which are symmetrical with respect to the trap centre $s = 0$. The decoupled, effective Hamiltonian is therefore

$$H'' = \sum_{\nu=\pm} \left[\frac{p_\nu^2}{2} + \frac{\Omega_\nu^2}{2} \left(s_\nu + \frac{p_{0\nu}}{\Omega_\nu^2} \right)^2 \right], \quad (21)$$

with

$$\begin{aligned} s_\pm &= \sqrt{\frac{m}{2}} \left[\left(s_1 + \frac{x_0}{2} \right) \mp \left(s_2 - \frac{x_0}{2} \right) \right], \\ p_{0+} &= -\sqrt{\frac{m}{2}} \dot{x}_0, \quad p_{0-} = 0, \\ \Omega_+^2 &= 3\omega^2, \quad \Omega_-^2 = \omega^2. \end{aligned} \quad (22)$$

We consider rotation protocols with a smooth behavior of θ at the boundary times $t_b = 0, t_f$,

$$\theta(0) = 0, \quad \theta(t_f) = \theta_f, \quad (23)$$

$$\dot{\theta}(t_b) = \ddot{\theta}(t_b) = 0. \quad (24)$$

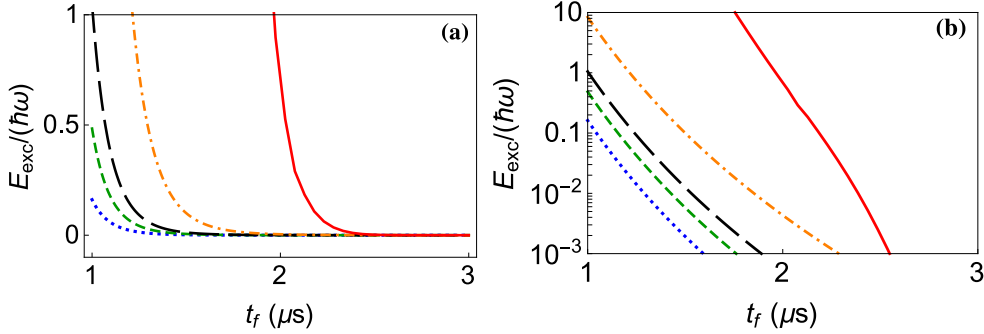


Figure 2. (Color online) Two equal ions. Exact energy excess (final minus initial energy) starting from the ground state and with dynamics driven by the full potential (16) according to equation (33) for the parameters c_{3-6} that minimise the excitation in the normal modes. (a) represents this excitation in a linear scale and (b) in a logarithmic scale. Dotted blue line: protocol using all 4 free parameters in the ansatz for $\theta(t)$; Short-dashed green line: only 3 free parameters, i.e., $c_6 = 0$; Long-dashed black line: only 2 free parameters, i.e., $c_5 = c_6 = 0$; Dash-dotted orange line: only one free parameter, i.e., $c_4 = c_5 = c_6 = 0$; Solid red line fixes: $c_{3-6} = 0$ so there is no optimisation. The evolution was done for two $^{40}\text{Ca}^+$ ions, with an external trap frequency $\omega_0/(2\pi) = 1.41$ MHz and a total rotation angle $\theta_f = \pi$.

These conditions imply that

$$\omega(t_b) = \omega_0, \quad (25)$$

$$\dot{\omega}(t_b) = \ddot{\omega}(t_b) = \dot{p}_{0\nu}(t_b) = 0. \quad (26)$$

The two independent harmonic oscillators expand or compress through the time dependence of Ω_ν and experiment a “transport”, in s_ν space, along $\dot{p}_{0\nu}/\Omega_\nu^2$. The Hamiltonian (21) has a dynamical invariant [34]

$$I = \sum_{\nu=\pm} \frac{1}{2} [b_\nu(p_\nu - \dot{\alpha}_\nu) - \dot{b}_\nu(s_\nu - \alpha_\nu)]^2 + \frac{1}{2} \Omega_{0\nu}^2 \left(\frac{s_\nu - \alpha_\nu}{b_\nu} \right)^2, \quad (27)$$

where $\Omega_{0\pm} = \Omega_\pm(0)$, and b_\pm (scaling factors of the normal mode wavefunctions) and α_\pm (reference classical trajectories for each oscillator) are auxiliary functions that have to satisfy, respectively, the Ermakov and Newton equations,

$$\ddot{b}_\pm + \Omega_\pm^2 b_\pm = \frac{\Omega_{0\pm}^2}{b_\pm^3}, \quad (28)$$

$$\ddot{\alpha}_\pm + \Omega_\pm^2 \alpha_\pm = \dot{p}_{0\pm}. \quad (29)$$

The time-dependent Schrödinger equation can be solved by superposing, with constant coefficients, elementary solutions which are also eigenstates of the invariant, with the (“Lewis-Riesenfeld”) phase adjusted to be also solutions of the Schrödinger equation [23],

$$|\psi''_{n\pm}\rangle = e^{\frac{i}{\hbar} \left[\frac{b_\pm s_\pm^2}{2b_\pm} + (\dot{\alpha}_\pm b_\pm - \alpha_\pm \dot{b}_\pm) \frac{s_\pm}{b_\pm} \right]} \frac{1}{\sqrt{b_\pm}} \Phi_n(\sigma_\pm), \quad (30)$$

where $\sigma_{\pm} = \frac{s_{\pm} - \alpha_{\pm}}{b_{\pm}}$ and Φ_n are the eigenfunctions for the static harmonic oscillators with frequencies $\Omega_{0,\pm}$. The average energies for the n th elementary solution of each mode can be calculated [29, 30],

$$\begin{aligned} E''_{n\pm} &= \langle \psi''_{n\pm} | H'' | \psi''_{n\pm} \rangle \\ &= \frac{(2n+1)\hbar}{4\Omega_{0\pm}} \left(\dot{b}_{\pm}^2 + \Omega_{\pm}^2 b_{\pm}^2 + \frac{\Omega_{0\pm}^2}{b_{\pm}^2} \right) + \frac{1}{2} \dot{\alpha}_{\pm}^2 + \frac{1}{2} \Omega_{\pm}^2 \left(\alpha_{\pm} - \frac{\dot{p}_{0\pm}}{\Omega_{\pm}^2} \right)^2. \end{aligned} \quad (31)$$

As $\dot{p}_{0\nu}(t_f) = 0$, the final values are minimised when the only contribution is due to the eigenenergies for the oscillators, with

$$b_{\pm}(t_f) = 1, \alpha(t_f) = \dot{\alpha}(t_f) = \dot{b}_{\pm}(t_f) = 0. \quad (32)$$

3.1. Inverse engineering

Imposing commutativity between Hamiltonian and invariant at initial $t = 0$ and final times $t = t_f$, the invariant drives the initial eigenstates of H to corresponding final eigenstates along the elementary solutions (30), although there could be diabatic excitations at intermediate times, when the commutation between Hamiltonian and invariant is not guaranteed. By inspection of equation (30), commutativity at the boundary times is achieved if the conditions in equation (32) are satisfied, which occur automatically when the final energies (31) are minimised. To inverse engineer the rotation we proceed similarly to reference [20], with an ansatz for $\theta(t)$ that satisfies boundary conditions (23) and (24) with some free parameters. We use up to 4 free parameters,

$$\begin{aligned} \theta(t) &= \frac{1}{16} (32c_3 + 80c_4 + 144c_5 + 224c_6 - 9\theta_f) \cos\left(\frac{\pi t}{t_f}\right) \\ &\quad - \frac{1}{16} (48c_3 + 96c_4 + 160c_5 + 240c_6 - \theta_f) \cos\left(\frac{3\pi t}{t_f}\right) \\ &\quad + c_3 \cos\left(\frac{5\pi t}{t_f}\right) + c_4 \cos\left(\frac{7\pi t}{t_f}\right) + c_5 \cos\left(\frac{9\pi t}{t_f}\right) + c_6 \cos\left(\frac{11\pi t}{t_f}\right) + \frac{\theta_f}{2}. \end{aligned} \quad (33)$$

This gives an expression of $\dot{\theta}$, from which we find ω in equation (19). We introduce ω in (22) to get the normal mode angular frequencies Ω_{\pm} needed in the Ermakov equation (28). For a given set of values of these parameters we solve the “direct problem” (Ermakov and Newton equations) with initial conditions

$$\begin{aligned} b_{\pm}(0) &= 1, \dot{b}_{\pm}(0) = 0, \\ \alpha_{\pm}(0) &= \dot{\alpha}_{\pm}(0) = 0, \end{aligned} \quad (34)$$

and compute easily the final energies with equation (31). The values of the parameters are varied with a subroutine that minimises the sum of the final mode energies (31) (we use the MatLab ‘fminsearch’ and $n = 0$ but note that the optimal final values of $b(t_f)$, $\alpha(t_f)$ and their derivatives would minimise the energies for any n). The excess energy found with the optimal parameters for the normal modes is negligible in the

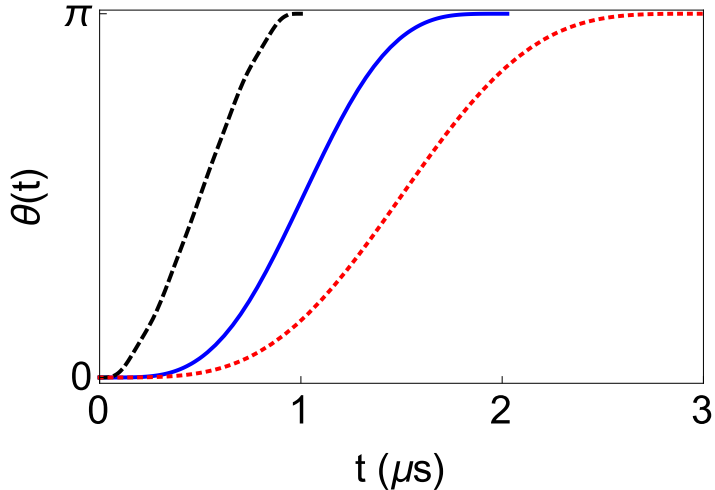


Figure 3. (Color online) Evolution of the control parameter $\theta(t)$ for different final times when designed using all 4 free parameters. Dashed black line: $t_f = 1 \mu\text{s}$, and optimisation parameters $c_{3-6} = (5.134, -5.360, 59.577, 91.234) \times 10^{-4}$; Solid blue line: $t_f = 2 \mu\text{s}$, and optimisation parameters $c_{3-6} = (3.093, 0.971, 3.386, -6.036) \times 10^{-4}$; Dotted red line: $t_f = 3 \mu\text{s}$, and optimisation parameters $c_{3-6} = (1.400, -0.270, 0.182, -0.117) \times 10^{-4}$. Other parameters as in figure 2.

range of final times depicted in figure 2. Once the free parameters are defined such that the design of θ minimises the excitation energy of the normal modes, we perform the quantum evolution driven by the full Hamiltonian with (16) to check the performance of the designed protocol. We use the “Split-Operator Method”, and the initial ground state is found performing an evolution in imaginary time. Figure 2 shows the final excitation, i.e., the excess energy with respect to the initial energy after performing the evolution with the full Hamiltonian (3) using the potential (16). In figure 2 (a) this excitation is depicted in a linear scale, and in figure 2 (b) in a logarithmic scale. The results improve significantly by using more optimisation parameters. Even when using a single optimising parameter, the results are clearly better than the protocol without free parameters. Figure 3 shows some examples of the rotation protocols with 4 parameters for different rotation times.

4. Two different ions

Let us first explore some possible manipulations to make the modes separable when the ions are different. From the expression of $\tan 2\mu$ in equation (18), d^3k should be constant. If the only parameter that depends on time is d , this condition cannot be satisfied. But if k is allowed to be a time dependent controllable parameter, it would be in principle possible. If we set the constant as B then, from equation (18), the relation

$$\tan 2\mu = \frac{4C_c\sqrt{m_1 m_2}}{(m_1 - m_2)(2C_c + B)}, \quad (35)$$

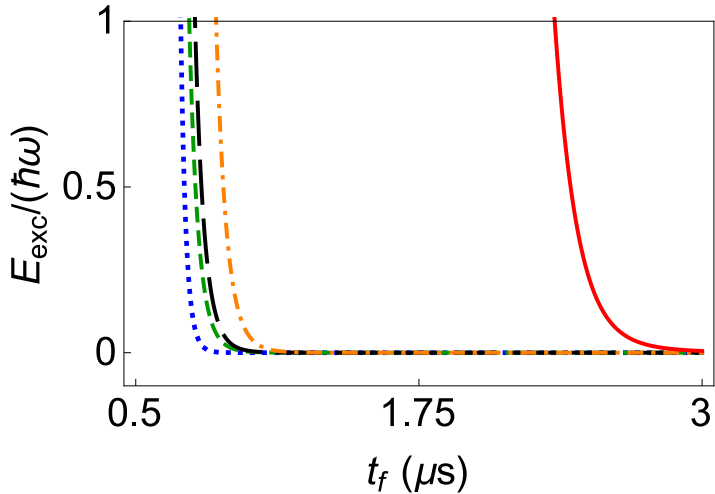


Figure 4. (Color online) Two different ions. Exact energy excess (final minus initial energy) when the initial ground state is driven by the full potential (16) according to equation (33) for the parameters c_{3-6} that minimise this excitation. Dotted blue line: protocol using all 4 free parameters in the ansatz for $\theta(t)$; Short-dashed green line: only 3 free parameters, i.e., $c_6 = 0$; Long-dashed black line: only 2 free parameters, i.e., $c_5 = c_6 = 0$; Dash-dotted orange line: only one free parameter, i.e., $c_4 = c_5 = c_6 = 0$; Solid red line fixes: $c_{3-6} = 0$ so there is no optimisation. The evolution was done for a $^{40}\text{Ca}^+$ and a $^9\text{Be}^+$ ion, with an external trap frequency for the Ca ion of $\omega_1/(2\pi) = 1.41$ MHz and a total rotation angle $\theta_f = \pi$.

fixes μ to have independent dynamical modes. Using the expressions for d and the u_i , this condition may be satisfied for two values of $\dot{\theta}^2 = a_l k$ for each k , $l = 1, 2$, where the a_l are two constants. The proportionality between $\dot{\theta}^2$ and k , however, is problematic. If we wish to approach $\dot{\theta} = 0$ smoothly at the time boundaries, then $k \rightarrow 0$ there, which implies a vanishing trapping potential and $d \rightarrow \infty$. A way out is explored in Appendix B making use of a more complex external trap potential with linear and quartic terms added, as in reference [31]. In the main text we stay within the harmonic trap configuration with constant k and renounce to separate the modes. Thus a different, pragmatic strategy is adopted, minimising the excitation energy directly to find the rotation protocol. We use the same ansatz for the parameter control θ as in equation (33) and solve the full (quantum) dynamics for the potential (16) to find the final excess energy for specific values of the free parameters c_{3-6} . Then, as in section 3.1, we minimise the excess energy letting the MATLAB subroutine ‘fminsearch’ find the optimal parameters.

In figure 4 we depict this final excitation, optimising the result using from 1 to 4 free parameters for the θ , and compare it with the results for no free parameters. This direct minimisation provides even better results than the indirect one based on the normal mode energy in section 3.1. The best protocol (4 optimising parameters) gives an excitation below 0.1 quanta at a final time $t_f = 0.56 \mu\text{s}$. The price to pay though, is that the computational time required increases dramatically, as we have to

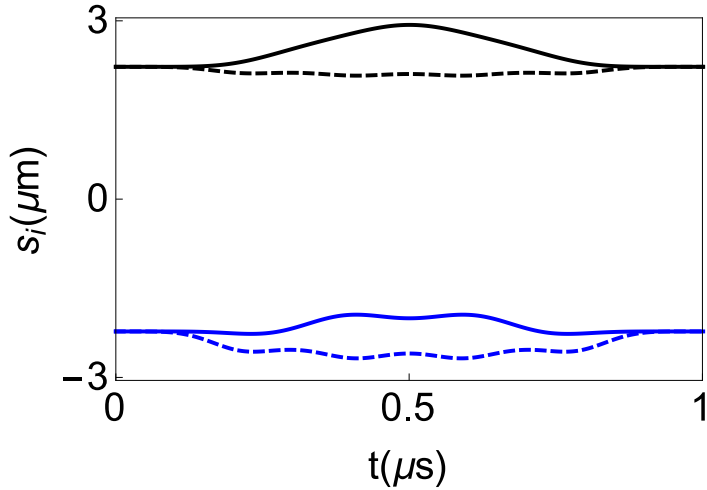


Figure 5. (Color online) Equilibrium (dashed lines) and dynamical (solid lines) positions of the ions versus time: $s_1^{(0)}$ and s_1 (Calcium ion, blue lines); $s_2^{(0)}$ and s_2 (Berillium ion, black lines), for a final time $t_f = 1 \mu\text{s}$ and for the optimising parameters $c_{3-6} = (1.757, 1.824, 1.120, -0.234) \times 10^{-2}$ with the protocol in equation (33). The initial state is the ground state. The s_i are average positions from the quantum dynamics.

solve the full dynamics of the system at every iteration of the shooting method we use to optimise, whereas in the method based on normal modes we only needed to solve four ordinary differential equations at each iteration. Figure 5 shows the equilibrium and dynamical positions of both ions during the evolution for $t_f = 1 \mu\text{s}$. The trajectories are not symmetric since the two ions experience different effective spring constants, see equation (17).

5. Discussion

We have designed protocols to rotate a linear trap containing two ions, without final excitation. For two equal ions in a rotating, rigid harmonic trap, there are uncoupled dynamical normal modes. The separation facilitates inverse engineering since it is only necessary to solve ordinary differential equations for independent variables to minimise the final energy. These Ermakov and Newton equations are for the auxiliary functions in the invariants associated with the uncoupled Hamiltonians. Following this method and for a given ansatz for the rotation angle and for some allowed final excitation threshold, process-time lower limits are met due to the eventual failure of the small oscillation regime for very rapid rotations. Faster processes can be achieved by increasing the number of parameters in the ansatz. For two different ions in a harmonic trap, this method is not possible as the modes are coupled for a rigid trap, or can be uncoupled for a non-rigid trap but only for impractical boundary conditions for the trap. Instead we used direct optimisation of the rotation ansatz parameters with the full Hamiltonian. This direct approach is efficient with respect to the lower time limits but the computational

effort is much more demanding.

A natural extension of this work would be considering different boundary conditions, for example a final rotating trap with $\dot{\theta}(t_f) \neq 0$, as in reference [16], to transfer an angular momentum to the chain. Another possible future extension would be adding noises and perturbations to make the protocols robust with respect to them. Finally, specific protocols could be designed to simultaneously rotate longer chains of ions, although it is possible to sequentially rotate them in groups of 2 using the protocols designed here.

Acknowledgements

We thank Uli Poschinger for discussions on the early stages of this paper. This work was supported by the Basque Country Government (Grant No. IT986-16), and by the Spanish Ministry of Science and Innovation through projects PGC2018-101355-B-I00 and PGC2018-095113-B-I00 (MCIU/AEI/FEDER,UE).

- [1] Palmero M, Martínez-Garaot S, Leibfried D, Wineland D J and Muga J G 2017 *Phys. Rev. A* **95**(2) 022328 URL <https://link.aps.org/doi/10.1103/PhysRevA.95.022328>
- [2] Campbell W C and Hamilton P 2017 *Journal of Physics B: Atomic, Molecular and Optical Physics* **50** 064002 URL <https://doi.org/10.1088/1361-6455/aa5a8f>
- [3] Martínez-Garaot S, Rodriguez-Prieto A and Muga J G 2018 *Phys. Rev. A* **98**(4) 043622 URL <https://link.aps.org/doi/10.1103/PhysRevA.98.043622>
- [4] Rodriguez-Prieto A, Martínez-Garaot S, Lizuain I and Muga J G 2020 *Phys. Rev. Research* **2**(2) 023328 URL <https://link.aps.org/doi/10.1103/PhysRevResearch.2.023328>
- [5] Kielpinski D, Monroe C and Wineland D J 2002 *Nature* **417** 709–11 ISSN 0028-0836 URL <http://dx.doi.org/10.1038/nature00784>
- [6] Rowe, M A; Ben-Kish, A; DeMarco, B; Leibfried, D; Meyer, V; Beall, J; Britton, J; Hughes, J; Itano, W M; Jelenkovic, B; Langer, C; Rosenband, T; and Wineland D J 2002 *Quantum Inf. Comput.* **2** 257
- [7] Reichle R, Leibfried D, Blakestad R, Britton J, Jost J, Knill E, Langer C, Ozeri R, Seidelin S and Wineland D 2006 *Fortschritte der Physik* **54** 666–685 ISSN 0015-8208 URL <http://doi.wiley.com/10.1002/prop.200610326>
- [8] Home J P, Hanneke D, Jost J D, Amini J M, Leibfried D and Wineland D J 2009 *Science (New York, N.Y.)* **325** 1227–30 ISSN 1095-9203 URL <http://www.sciencemag.org/content/325/5945/1227>
- [9] Roos C 2012 *Physics* **5** URL <http://physics.aps.org/articles/v5/94>
- [10] Monroe C and Kim J 2013 *Science (New York, N.Y.)* **339** 1164–9 ISSN 1095-9203 URL <http://www.sciencemag.org/content/339/6124/1164>
- [11] Kaushal V, Lekitsch B, Stahl A, Hilder J, Pijn D, Schmiegelow C, Bermudez A, Müller M, Schmidt-Kaler F and Poschinger U 2020 *AVS Quantum Science* **2** 014101 (Preprint <https://doi.org/10.1116/1.5126186>) URL <https://doi.org/10.1116/1.5126186>
- [12] Wan Y, Jördens R, Erickson S D, Wu J J, Bowler R, Tan T R, Hou P Y, Wineland D J, Wilson A C and Leibfried D 2020 *Advanced Quantum Technologies* **3** 2000028 (Preprint <https://onlinelibrary.wiley.com/doi/pdf/10.1002/qute.202000028>) URL <https://onlinelibrary.wiley.com/doi/abs/10.1002/qute.202000028>
- [13] Splatt F, Harlander M, Brownnutt M, Zähringer F, Blatt R and Hänsel W 2009 *New Journal of Physics* **11** 103008 ISSN 1367-2630 URL <http://stacks.iop.org/1367-2630/11/i=10/a=103008?key=crossref.9fb433c77b780aa19045455cad9508b3>
- [14] Kaufmann H, Ruster T, Schmiegelow C T, Luda M A, Kaushal V, Schulz J, von

Lindenfels D, Schmidt-Kaler F and Poschinger U G 2017 *Phys. Rev. A* **95**(5) 052319 URL <https://link.aps.org/doi/10.1103/PhysRevA.95.052319>

[15] Horstmann B, Reznik B, Fagnocchi S and Cirac J I 2010 *Phys. Rev. Lett.* **104**(25) 250403 URL <https://link.aps.org/doi/10.1103/PhysRevLett.104.250403>

[16] Urban E, Glikin N, Mouradian S, Krimmel K, Hemmerling B and Haeffner H 2019 *Physical Review Letters* **123** URL <https://doi.org/10.1103/physrevlett.123.133202>

[17] Roos C F, Alberti A, Meschede D, Hauke P and Häffner H 2017 *Phys. Rev. Lett.* **119**(16) 160401 URL <https://link.aps.org/doi/10.1103/PhysRevLett.119.160401>

[18] Masuda S and Rice S A 2015 *Journal of Physical Chemistry B* **119** 11079–11088 URL <https://doi.org/10.1021/acs.jpcb.5b02681>

[19] van Mourik M W, Martinez E A, Gerster L, Hrmo P, Monz T, Schindler P and Blatt R 2020 *Phys. Rev. A* **102**(2) 022611 URL <https://link.aps.org/doi/10.1103/PhysRevA.102.022611>

[20] Palmero M, Wang S, Guéry-Odelin D, Li J S and Muga J G 2016 *New Journal of Physics* **18** 043014 ISSN 1367-2630 URL <http://stacks.iop.org/1367-2630/18/i=4/a=043014?key=crossref.d167da0474c8485c86186bc30430d9e1>

[21] Lizuain I, Palmero M and Muga J G 2017 *Phys. Rev. A* **95**(2) 022130 URL <https://link.aps.org/doi/10.1103/PhysRevA.95.022130>

[22] Guéry-Odelin D, Ruschhaupt A, Kiely A, Torrontegui E, Martínez-Garaot S and Muga J G 2019 *Rev. Mod. Phys.* **91**(4) 045001 URL <https://link.aps.org/doi/10.1103/RevModPhys.91.045001>

[23] Torrontegui E, Ibáñez S, Chen X, Ruschhaupt A, Guéry-Odelin D and Muga J G 2011 *Physical Review A* **83** 013415 ISSN 1050-2947 URL <http://link.aps.org/doi/10.1103/PhysRevA.83.013415>

[24] Palmero M, Torrontegui E, Guéry-Odelin D and Muga J G 2013 *Physical Review A* **88** 053423 ISSN 1050-2947 URL <http://link.aps.org/doi/10.1103/PhysRevA.88.053423>

[25] Palmero M, Bowler R, Gaebler J P, Leibfried D and Muga J G 2014 *Physical Review A* **90** 053408 ISSN 1050-2947 URL <http://link.aps.org/doi/10.1103/PhysRevA.90.053408>

[26] Lu X J, Muga J G, Chen X, Poschinger U G, Schmidt-Kaler F and Ruschhaupt A 2014 *Physical Review A* **89** 063414 ISSN 1050-2947 URL <http://link.aps.org/doi/10.1103/PhysRevA.89.063414>

[27] Lu X J, Palmero M, Ruschhaupt A, Chen X and Muga J G 2015 *Physica Scripta* **90** 074038 ISSN 0031-8949 URL <http://stacks.iop.org/1402-4896/90/i=7/a=074038?key=crossref.11ad94fde3012bbc4a34ea49e8ac4b54>

[28] Chen X, Ruschhaupt A, Schmidt S, del Campo A, Guéry-Odelin D and Muga J G 2010 *Physical Review Letters* **104** 063002 ISSN 0031-9007 URL <https://link.aps.org/doi/10.1103/PhysRevLett.104.063002>

[29] Palmero M, Martínez-Garaot S, Alonso J, Home J P and Muga J G 2015 *Physical Review A* **91** 053411 ISSN 1050-2947 URL <http://link.aps.org/doi/10.1103/PhysRevA.91.053411>

[30] Palmero M, Martínez-Garaot S, Poschinger U G, Ruschhaupt A and Muga J G 2015 *New Journal of Physics* **17** 093031 ISSN 1367-2630 URL <http://stacks.iop.org/1367-2630/17/i=9/a=093031?key=crossref.f41a7e24866b757db75c22e80d245724>

[31] Sägesser T, Matt R, Oswald R and Home J P 2020 *New Journal of Physics* **22** 073069 URL <https://doi.org/10.1088/1367-2630/ab9e32>

[32] Lizuain I, Tobalina A, Rodriguez-Prieto A and Muga J G 2019 *Journal of Physics A: Mathematical and Theoretical* **52** 465301 URL <https://doi.org/10.1088/1751-8121/ab4a2f>

[33] Kaufmann P, Gloger T F, Kaufmann D, Johanning M and Wunderlich C 2018 *Phys. Rev. Lett.* **120**(1) 010501 URL <https://link.aps.org/doi/10.1103/PhysRevLett.120.010501>

[34] Lewis H R and Riesenfeld W B 1969 *Journal of Mathematical Physics* **10** 1458 ISSN 00222488 URL <http://scitation.aip.org/content/aip/journal/jmp/10/8/10.1063/1.1664991>

[35] Martínez-Garaot S, Palmero M, Guéry-Odelin D and Muga J G 2015 *Phys. Rev. A* **92**(5) 053406 URL <https://link.aps.org/doi/10.1103/PhysRevA.92.053406>

Appendix A. Magnetic force vs electric force

Two charged particles moving in a direction perpendicular to the direction in which they are aligned experience a magnetic force, with magnitude

$$F_{mag} = \frac{\mu_0 e^2}{4\pi r^2} |\vec{v}_1 \times (\vec{v}_2 \times \hat{r})|, \quad (\text{A.1})$$

where μ_0 is the permeability constant, \vec{v}_i the velocity vectors of each ion, $\vec{r} = \vec{s}_2 - \vec{s}_1$ the position vector of ion 2 with reference to ion 1, and $\hat{r} = \vec{r}/r$. The Coulomb interaction, which is the only one considered so far, gives a force of magnitude

$$F_{el} = \frac{C_c}{r^2}. \quad (\text{A.2})$$

The ratio of these two forces is, using $\mu_0\epsilon_0 = c^{-2}$, where c is the speed of light,

$$R = \frac{F_{mag}}{F_{el}} = \frac{|\vec{v}_1 \times (\vec{v}_2 \times \hat{r})|}{c^2}. \quad (\text{A.3})$$

With $|\vec{v}_1|, |\vec{v}_2| \approx \frac{r}{2}\dot{\theta}$ we get

$$R \approx \frac{r^2\dot{\theta}^2}{4c^2}. \quad (\text{A.4})$$

For the protocols designed in the main text, the maximum values during the simulations at the represented times are $\dot{\theta}_{max} = 5 \times 10^6 \text{ s}^{-1}$ and $r_{max} = 5.5 \times 10^{-6} \text{ m}$ so the magnetic interaction is negligible with respect to the electric force.

Appendix B. Rotation of two different species ions based on dynamical normal modes

If the matrix \mathbf{v} is time dependent, the normal modes get decoupled if $v_{11} = v_{22}$, see equation (8), i.e.,

$$\frac{1}{m_1} \frac{\partial^2 V}{\partial s_1^2} \Big|_{s_1^{(0)}} = \frac{1}{m_2} \frac{\partial^2 V}{\partial s_2^2} \Big|_{s_2^{(0)}}. \quad (\text{B.1})$$

As explained in the main text, the rotation of different ions trapped by a rigid harmonic potential cannot be described in general in terms of dynamical normal modes. For a non-rigid one there is a formal solution which does not lead to practically useful boundary conditions. Here we consider different confining potentials that obey equation (B.1), and thus allow us to inverse engineer the rotation using the Lewis-Riesenfeld family of invariants. We use for the equilibrium positions the parametrisation $s_1^{(0)} = s_0 - d/2$ and $s_2^{(0)} = s_0 + d/2$, where s_0 is the middle point between them.

Specifically we consider a tilted double well potential, which combines a repulsive harmonic potential with the confinement provided by the quartic term and a linear term [31],

$$V = \gamma(t)(s_1 + s_2) + \frac{1}{2}u_1(t)s_1^2 + \frac{1}{2}u_2(t)s_2^2 + \beta(s_1^4 + s_2^4) + \frac{C_c}{s_2 - s_1}. \quad (\text{B.2})$$

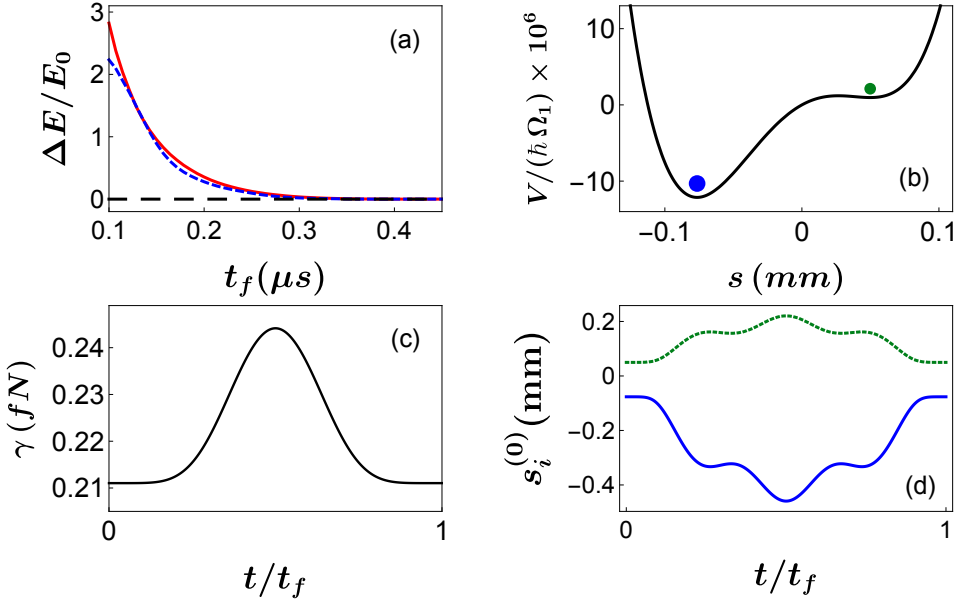


Figure B1. (a) Normal mode excitation $\Delta E = E(t_f) - E(0)$ in units of the initial energy $E_0 \equiv E(0)$ for different final times. The protocol rotates a $^{40}\text{Ca}^+$ and a $^9\text{Be}^+$ ion in a double well potential with $m_1\omega_1^2 = m_2\omega_2^2 = -4.7 \text{ pN/m}$ and $\beta = 0.52 \text{ mN/m}^3$. The initial state is a product of the ground states of each normal mode and thus, the energy of the system is computed as $E = E''_+ + E''_-$, see equation (31). The solid red line represents a non-optimised protocol; blue dotted and black dashed and lines represent optimised protocols using one and two parameters respectively. (b) Initial potential configuration and (c) the required $\gamma(t)$, see equation (B.6), for the protocol with two optimisation parameters ($c_3 = 0.0059$ and $c_4 = 0.0285$) and $t_f = 1 \mu\text{s}$. (d) Corresponding evolution of the equilibrium positions, whose initial value is also represented in (b). The blue solid line is for $^{40}\text{Ca}^+$ and the green dashed line for $^9\text{Be}^+$.

This gives the potential matrix

$$\mathbf{v} = \begin{pmatrix} \frac{\frac{2C_c}{d^3} + u_1 + 12\left(-\frac{d}{2} + s_0\right)^2\beta}{m_1} & -\frac{2C_c}{d^3\sqrt{m_1 m_2}} \\ -\frac{2C_c}{d^3\sqrt{m_1 m_2}} & \frac{\frac{2C_c}{d^3} + u_2 + 12\left(\frac{d}{2} + s_0\right)^2\beta}{m_2} \end{pmatrix}. \quad (\text{B.3})$$

The main-text equations from equation (7) to (15) are still valid here. We assume that the controllable parameters are the linear potential and the rotation speed. Equation (B.1) is satisfied whenever d obeys

$$\left\{ A(m_1 - m_2)(u_1 - u_2) + d^2 \left[6A\beta(m_1 + m_2) + (m_1 - m_2)(u_1 - u_2)^2 \right] + 24\beta C_c d(m_1 - m_2) + 12\beta^2 d^6(m_1 - m_2) \right\} = 0, \quad (\text{B.4})$$

where we have defined

$$A = \sqrt{d^3[24\beta C_c - 12\beta^2 d^5 - 12\beta d^3(u_1 + u_2) + d(u_1 - u_2)^2]}. \quad (\text{B.5})$$

The force $\gamma(t)$ that would produce the desired evolution for d is

$$\gamma = \frac{1}{108\beta^2 d^6} \left\{ 18\beta C_c d^2(u_2 - u_1) - 24\beta^2 d^5 A - d(u_1 - u_2)^2 A \right\}$$

$$- 6\beta C_c A + 36\beta^2 d^7 (u_1 - u_2) + d^3 \left[-6\beta A(u_1 + u_2) - (u_1 - u_2)^3 \right] \}, \quad (B.6)$$

and the corresponding evolution for the middle point between the ions is

$$s_0 = \frac{A + d^2(u_1 - u_2)}{12\beta d^3}. \quad (B.7)$$

The frequencies of the normal modes Ω_{\pm} can be analytically expressed in terms of d , the parameters that define the potential (u_1 , u_2 and β) and the masses m_1 and m_2 , but they are too lengthy to be reproduced here. Provided that equation (B.4) is satisfied, the rotation of the potential in equation (B.2) is governed by an uncoupled Hamiltonian of the form (21), with the corresponding frequencies Ω_{\pm} and momentum shifts that read

$$p_{0\pm} = \frac{1}{\sqrt{2}} \left[(\sqrt{m_1} \pm \sqrt{m_2})\dot{s} + (\sqrt{m_2} \mp \sqrt{m_1})\frac{\dot{d}}{2} \right]. \quad (B.8)$$

From here on the procedure to design the protocol is similar to the one explained in section 3.1. We start from the same ansatz for $\theta(t)$, see equation (33), which satisfies the boundary conditions (23) and (24) by design, and search for the values of the free parameters that minimise the final excitation. Decoupling the dynamics of the system into independent dynamical normal modes, however, is more demanding here than for equal ions. We compute the necessary force, see equation (B.6), and equilibrium positions, see Eqs. (B.4) and (B.7), for each test value of the free parameters in $\theta(t)$.

Figure B1(a) shows that, for a rotation of a $^{40}\text{Ca}^+$ and a $^9\text{Be}^+$ ion chain, any of the protocols produce no excitations in the normal modes for processes as fast as 0.4 μs . It also illustrates the improvement of the results by increasing the number of free parameters for $\theta(t)$. Normal mode excitation is an approximation of the exact excitation, nevertheless, our results suggest that performing the rotation with the double well may provide excitationless protocols at short time scales.

Figure B1(b) and (c) depict, respectively, the initial potential and the required force $\gamma(t)$ for a specific rotation protocol using the tilted double well potential in equation (B.2). Notice that even the lowest value of the force, at boundary times, produces a considerable bias with little to none barrier potential between the two wells. Despite this, each equilibrium position, whose evolution is depicted in figure B1(c), initially lays in its own well. This unusual potential shape would be the price to pay for mode separability. We note that a potential bias may be imposed or cancelled using STA methods as well [35].